DOI: 10.1002/chem.200601161

2,2′-Biphosphinines and 2,2′-Bipyridines in Homoleptic Dianionic Group 4 Complexes and Neutral 2,2′-Biphosphinine Group 6 d^6 Metal Complexes: Octahedral versus Trigonal-Prismatic Geometries

Hervé Lesnard,[a, b] Thibault Cantat,[c] Pascal Le Floch,[c] Isabelle Demachy,*[a, b] and Yves Jean*[c]

Abstract: The geometric and electronic structure of formally d^6 tris-biphosphinine $[M(bp)_3]^q$ and tris-bipyridine $[M(bpy)_3]^q$ complexes were studied by means of DFT calculations with the B3LYP functional. In agreement with the available experimental data, Group 4 dianionic $[M(bp)_3]^{2-}$ complexes (**1P–3P** for M = Ti, Zr, and Hf, respectively) adopt a trigonal-prismatic (TP) structure, whereas the geometry of their nitrogen analogues $[M(bpy)_3]^{2-}$ (**1N–3N**) is nearly octahedral (OC), although a secondary minimum was found for the TP structures (**1N′–3N′**). The electronic factors at work in these systems are discussed by means of an MO analysis of the minima, MO correlation diagrams, and thermodynamic cycles connecting the octahedral and trigonal-prismatic limits. In all these complexes, pronounced electron transfer from the metal center to the lowest lying π* ligand orbitals makes the d^6 electron count purely formal. However, it is shown that the bp and bpy ligands accommodate the release of electron density from the metal in different ways because of a change in the localization of the HOMO, which is a mainly metal-centered orbital in bp complexes and a pure π* ligand orbital in bpy complexes. The energetic evolution of the HOMO allows a simple rationalization of the progressive change from the TP to the OC structure on successive oxidation of the $[Zr(bp)_3]^{2-}$ complex, a trend in agreement with the experimental structure of the monoanionic complex. The geometry of Group 6 neutral complexes $[M(bp)_3]$ (**4P** and **5P** for M = Mo and W, respectively) is found to be intermediate between the TP and OC limits, as previously shown experimentally for the tungsten complex. The electron transfer from the metal center to the lowest lying π* ligand orbitals is found to be significantly smaller than for the Group 4 dianionic analogues. The geometrical change between $[Zr(bp)_3]^{2-}$ and $[W(bp)_3]$ is analyzed by means of a thermodynamic cycle and it is shown that a larger ligand–ligand repulsion plays an important role in favoring the distortion of the tungsten complex away from the TP structure.

Keywords: chelates · density functional calculations · electronic structure · N ligands · P ligands · transition metals

Introduction

2,2′-Bipyridine (bpy) and derivatives are among the most studied ligands in the coordination chemistry of nitrogen compounds.[1] They have found many applications as elementary building blocks in supramolecular chemistry for the elaboration of various sophisticated rigid and flexible structures and devices such as helical assemblies,[2] chiral molecular recognition,[3,4] luminescent devices,[5,6] photonics and optoelectronics,[7] molecular grids,[8–10] knots and catenanes, and molecular motors[11–14] On the other hand, the presence of a low-lying π* system associated with their aromatic backbone has been extensively exploited to promote redox processes in transition-metal complexes. Thus polypyridyl complexes of d^6 metals such as Fe^{II}, Ru^{II}, and Os^{II} have at-

[a] H. Lesnard, Prof. I. Demachy
Université Paris-Sud
UMR 8000, Orsay, 91405 (France)
E-mail: demachy@lcp.u-psud.fr

[b] H. Lesnard, Prof. I. Demachy
CNRS, Orsay, 91405 (France)
Fax: (+33) 1-6915-6188

[c] T. Cantat, Prof. P. Le Floch, Prof. Y. Jean
Laboratoire "Hétéroéléments et Coordination"
École Polytechnique, CNRS
91128 Palaiseau (France)
Fax: (+33) 1-6933-3990
E-mail: yves.jean@polytechnique.fr

Supporting information for this article is available on the WWW under http://www.chemeurj.org/ or from the author.

tracted particular attention due to a combination of favorable photophysical and redox characteristics and the longevity of their excited states.[15] Furthermore, another important characteristic of bipyridines is their chemical inertness in a variety of oxidation states.

The replacement of nitrogen by phosphorus in similar structures has strongly attracted the interest of phosphorus chemists due to the marked difference that exists between two-coordinate phosphorus and nitrogen atoms.[16–18] The first semi-analogue of bipyridine with one phosphorus atom, 2-pyridyl-2-phosphinine (NIPHOS), was synthesized by Mathey et al.[19,20] Some studies were devoted to the coordination chemistry of this interesting ligand, but it rapidly became obvious that the presence of two electronically different atoms in the same structure made it difficult to handle;[21,22] the phosphorus atom of phosphinines is highly sensitive towards nucleophilic attack, whereas the nitrogen atom of pyridines is easily protonated.[23] A few years ago, we developed several synthetic routes towards 2,2′-biphosphinines (bp), which are exact phosphorus analogues of bipyridines.[24–29] These ligands with two two-coordinate phosphorus atoms exhibit electronic properties which markedly differ from those of their nitrogen counterparts. Indeed the replacement of nitrogen by two weakly electronegative phosphorus atoms results in a significant increase of the π-accepting capacity of the aromatic backbone. Electrochemical measurements have shown that the LUMO of the parent biphosphinine ($C_{10}H_8P_2$) lies 0.5 V lower than that of 2,2′-bipyridine.[30]

Thus, not surprisingly, biphosphinines proved to be very efficient ligands for the stabilization of electron-rich and even electron-excessive metal centers. Several anionic biphosphinine metal complexes were successfully synthesized and structurally characterized with Group 4,[31] 6,[32] 7,[33,34] 8,[35–41] 9[41,42] and 10[41,43,44] metals. During our studies on the synthesis of homoleptic Group 4 dianionic complexes of general formula $[M(bp)_3]^{2-}$ (M = Ti, Zr, Hf), we were interested in a comparison between the respective π-accepting capacities of biphosphinines and their bipyridine analogues. The synthesis of dianionic bipyridine complexes was initially investigated by Herzog et al. in the 1960s.[45] Comparison between the two types of ligands in such complexes proved to be difficult in the absence of theoretical data, and our analysis was only based on the examination of the internal C–C bond between the two aromatic subunits and the overall geometry of the complex. The first criterion has often been employed to assess the degree of delocalization within bipyridine and biphosphinine complexes, since the LUMO of both ligands has the same symmetry. In accord with the shape of these molecular orbitals, which are bonding between the two concerned carbon atoms (see Scheme 1), significant delocalization of electron density within the two rings should result in significant shortening of this intracyclic C–C bond. Finally, the coefficients on the heteroatoms in the LUMO are larger for bp than for bpy (Scheme 1), a factor which contributes to making the former a better π acceptor.

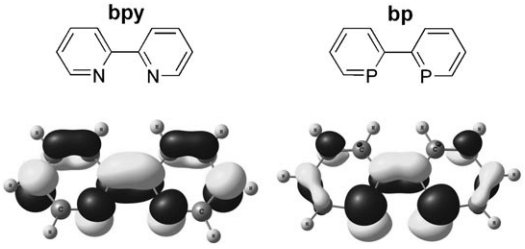

Scheme 1. LUMOs of bipyridine (bpy) and biphosphinine (bp) ligands for which a planar geometry has been assumed.

Abstract in French: *La structure électronique des complexes tris-biphosphinine $[M(bp)_3]^q$ et tris-bipyridine $[M(bpy)_3]^q$, présentant formellement une configuration électronique d^6, a été étudiée par des calculs DFT en utilisant la fonctionnelle B3LYP. En accord avec les données expérimentales disponibles, il a été montré que les complexes dianioniques du groupe 4 de formule générale $[M(bp)_3]^{2-}$ (**1P–3P** avec respectivement M = Ti, Zr, Hf) adoptent une structure trigonale prismatique (TP) alors que leurs analogues azotés $[M(bpy)_3]^{2-}$ (**1N–3N**) adoptent une géométrie de type octaédrique. Pour ces derniers, un minimum secondaire de structure trigonale prismatique a également été déterminé (**1N′–3N′**). Les facteurs électroniques intervenant dans ces différents systèmes sont discutés sur la base d'une analyse orbitalaire des minima, de diagrammes de corrélation et d'un cycle thermodynamique connectant les deux structures limites, octaédrique et trigonale prismatique. Dans tous ces complexes, il y a un important transfert électronique du métal vers les orbitales π* des ligands ce qui indique que le décompte électronique d^6 est purement formel. Il a cependant été montré que les ligands biphosphinine et bipyridine accommodent l'excès de densité électronique en provenance du métal d'une façon différente en raison d'un changement de localisation de la HOMO qui est principalement centrée sur le métal dans les complexes phosphorés et totalement centrée sur les ligands (système π*) dans les complexes de bipyridine. L'évolution énergétique de la HOMO permet de rationaliser le passage de la structure trigonale prismatique vers une structure de type octaédrique par oxydations successives du complexe $[Zr(bp)_3]^{2-}$. Cette prédiction théorique est en bon accord avec la structure expérimentale du monoanion. La géométrie des complexes du groupe 6 de type $[M(bp)_3]$ (**4P** et **5P** pour respectivement M = Mo et W) est intermédiaire entre trigonale prismatique et octaédrique, en bon accord avec les résultats expérimentaux pour le complexe du tungstène. Le transfert électronique du métal vers le système π* du ligand biphosphinine est plus faible que dans le cas des dérivés du groupe 4. Le changement de géométrie entre les complexes $[Zr(bp)_3]^{2-}$ et $[W(bp)_3]$ a été analysé au moyen d'un cycle thermodynamique qui permet de montrer que la répulsion entre ligands contribue fortement à destabiliser la structure trigonale prismatique dans le cas du tungstène.*

Contrary to expectation on the grounds of the relative π-accepting capacities of bp and bpy ligands, experimental data for the zirconium complexes revealed that bipyridine complexes can be described as the coordination of three bipyridine dianions to a Zr^{IV} center, while in biphosphinine complexes the electron density was found to be mainly delocalized between the metal and the ligands.[31] Thus in the $[Zr(bpy)_3]^{2-}$ complex the internal C–C distance was close to that expected for a C=C bond (1.36(1) Å), whereas the corresponding bond in $[Zr(bp)_3]^{2-}$ was found to be longer (1.434(4) Å) and suggests weaker π backdonation from the metal. Another important piece of information is the overall geometry of these homoleptic complexes. Whereas in bipyridine complexes the overall geometry around the metal center was found to be nearly octahedral (OC), biphosphinine derivatives adopted a trigonal-prismatic (TP) geometry (Scheme 2), which is unexpected for d^6 metal complexes.

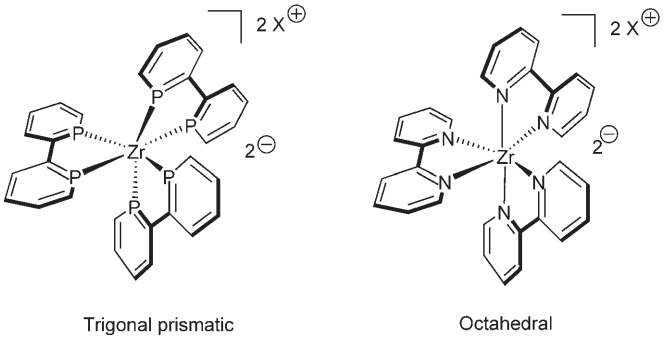

Scheme 2. Geometries of $[Zr(bp)_3]^{2-}$ and $[Zr(bpy)_3]^{2-}$.

The problem of the preference for TP geometry in d^6 biphosphinine complexes is not totally unprecedented, and DFT calculations were previously performed on a model of the neutral $[W(bp)_3]$ complex, which adopts an intermediate structure between the TP and OC limits.[32] These calculations, carried out by using a diphosphabutadiene (HP=CHCH=PH) as ligand in place of bp, revealed that this species was closer to a d^0 complex (with three dianionic ligands) than to a d^6 complex (three neutral ligands).[32] Note that a similar conclusion was drawn for the tris(butadiene)-molybdenum complex, which adopts a TP geometry.[46] On the basis of DFT and MP2 calculations and NBO analysis it was concluded that this complex was closer to a d^2 complex (Mo^{IV}) than to a genuine d^6 species. This conclusion led us to conclude that biphosphinines can not be simply considered as classical phosphine ligands and are related to noninnocent ligands such as dithiolenes, catecholates, *o*-quinones, and related species.[47–49]

All these data prompted us to investigate the problem of the electronic structure of these bipyridine and biphosphinine complexes. Herein we report on results of DFT calculations on Group 4 $[M(L–L)_3]^{2-}$ complexes (L–L = unsubstituted bpy and bp ligands, M = Ti, Zr, and Hf) and on Group 6 $[M(bp)_3]$ complexes (M = Mo and W). The main points addressed in this paper are the following: 1) What is the geometrical structure predicted for these complexes, some of which are known experimentally, but others not? 2) Why do the electronic structure and the geometry of Group 4 complexes depend on the nature of the ligands (bp or bpy)? 3) Which factors may be invoked to explain the geometrical change on going from Group 4 to Group 6 tris-biphosphinine complexes? In the following, the electronic factors at work in these systems are discussed by means of molecular orbital (MO) analysis of the minima and MO correlation diagrams between the OC and TP limits. Thermodynamic cycles are used to estimate the role played by other factors, such as ligand–ligand repulsion, in fixing the equilibrium geometry of these complexes.

Results and Discussion

Trigonal-prismatic versus octahedral geometries in homoleptic d^6 complexes: The basic orbital correlation diagram associated with the trigonal twist connecting the OC and TP structures has been derived by Hoffmann et al. for the d block (Scheme 3) in the absence of π interactions between

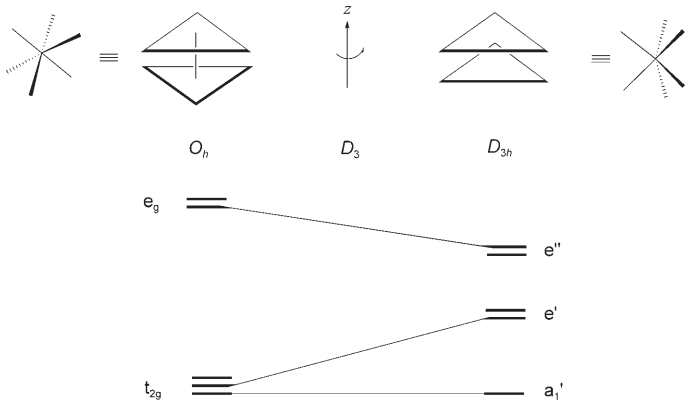

Scheme 3.

metal and ligands ($[CrH_6]^{6-}$ was used as model).[50] In this diagram, the highest possible symmetry for the limit (O_h and D_{3h}) and for the intermediate structures (D_3) was assumed. One of the t_{2g} components of the octahedron (z^2) is left unaffected, since the twisting ligands are on the nodal surface of z^2, and becomes a_1' in the D_{3h} TP structure. The other t_{2g} components are destabilized (e′ in D_{3h}) because they can now develop antibonding σ interactions with the ligands (their bonding counterpart, below the d-block orbitals, is stabilized). Finally, the set of e_g orbitals, which becomes e″ in D_{3h}, is stabilized by the decreased σ antibonding interactions with the ligands. The preference for the TP structure of a large number of electron-deficient compounds with d^0, d^1, and d^2 electronic configuration[51–53] can be rationalized neither by ligand–ligand repulsion, which is weaker in the octahedral structure, nor by the d-block

energy since the lowest lying d orbital remains unperturbed (Scheme 3). However, better metal–ligand σ bonding works in favor of the TP structure[50,52,53] since four d orbitals (e′ and e″) are involved instead of two in the octahedron (e_g). On the other hand, the OC structure of most of the low-spin d^6 complexes is readily rationalized by Scheme 3, since four of the six d electrons would be destabilized in the TP structure.

Hoffmann et al. have shown that distortion of such d^6 complexes away from their usual octahedral structure can be favored by strong π backbonding interactions with the ligands.[50] In the case of three chelate ligands carrying a low-lying π* orbital locally symmetric on the binding sites, the three π* acceptor orbitals transform as a_2' and e′ if D_{3h} symmetry is assumed for the TP structure.[54] The d-block antibonding e′ orbitals can therefore be stabilized by interacting with the π*(e′) vacant orbitals of the ligands, so that distortion toward the TP structure might be favored even for a d^6 electronic configuration. A consequence of these d–π* interactions is pronounced metal→ligands electron transfer, which makes the metal center poorer in electrons than expected from the formal electron count. In this context, bipyridine (bpy) and its phosphorus analogue biphosphinine (bp) are nice candidates to stabilize the TP structure in d^6 complexes. In fact, both carry a low-lying π* acceptor orbital, symmetric on the binding sites (Scheme 1).

Computational details: The distortion from the octahedron was expressed in terms of the trigonal twist angle θ, defined as the angle between the medians of the two appropriate trigonal faces (Scheme 4). For monodentate ligands, $\theta = 60°$

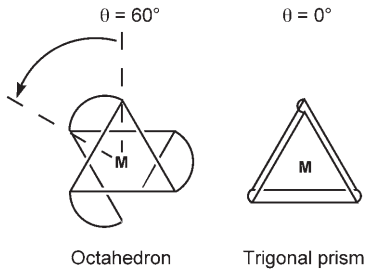

Scheme 4.

and $\theta = 0°$ denote the ideal OC and TP limits, respectively. For three chelate ligands with bite angles b smaller than 90°,[55,56] $\theta = 0°$ still applies to the trigonal prism but the octahedral limit corresponds to θ values smaller than 60° (48.2 and 36.0° for $b = 80$ and 70°, respectively).[56]

Another consequence of the presence of chelate ligands is that the O_h symmetry cannot be reached for the OC structure. The available symmetries are only D_3 and C_3 and the same holds for intermediate structures with $\theta \neq 0°$. For the TP structure ($\theta = 0°$), the D_{3h} symmetry is available, as well as lower C_{3h}, D_3, and C_3 symmetries. In our calculations, the minima were optimized without symmetry constraints (C_1), but their geometries were generally found to be very close to one of the above-mentioned symmetries. Therefore, the associated symmetry labels were used to simplify the analysis of the orbital interactions which develop between the metal and the ligands.

Calculations were performed with the Gaussian 03 series of programs.[57] Density functional theory (DFT)[58,59] was applied with the B3LYP functional.[60–62] A quasirelativistic effective core potential operator was used to represent the 10 innermost electrons of the titanium atom, the 28 innermost electrons of the zirconium and molybdenum atoms, the 60 innermost electrons of the hafnium and tungsten atoms,[63] as well as the electron core of the P atoms.[64] The basis set for the metal atoms was that associated with the pseudopotential, with a standard double-ζ LANL2DZ contraction.[63] The basis set for the P atoms was that associated with the pseudopotential, with a standard double-ζ LANL1DZ contraction[64] supplemented with a set of d-polarization functions.[65] The 6-31G* basis set was used for N atoms, and the 6-31G basis set for C and H atoms.[66,67] The stationary points were characterized as minima or transition states by frequency calculations. The decomposition of MOs into metal and ligand fragment orbitals was performed with the AOMIX program developed by Gorelsky and Lever, whereby the metal fragment is dianionic (M = Ti, Zr and Hf) or neutral (M = Mo and W) and the set of the three ligands (bp or bpy) neutral.[68,69]

Optimized geometries, energies, and frequencies of **1P–5P**, **1N–3N**, **1N′–3N′**, $[Zr(bp)_3]^-$, and $[Zr(bp)_3]$ are available as Supporting Information.

Group 4 complexes

Geometrical structures of the minima: The optimized structures of $[M(bp)_3]^{2-}$ (**1P–3P**) and $[M(bpy)_3]^{2-}$ (**1N–3N**) complexes with M = Ti, Zr, and Hf, respectively, are shown in Figure 1, and the main theoretical parameters are given in

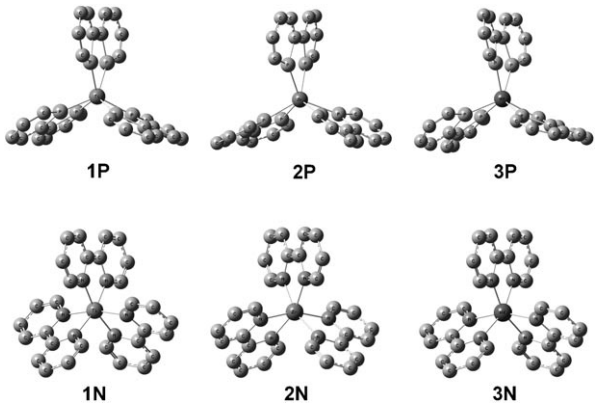

Figure 1. Optimized geometries of $[M(bp)_3]^{2-}$ complexes (M = Ti (**1P**), Zr (**2P**), and Hf (**3P**)) and $[M(bpy)_3]^{2-}$ complexes (M = Ti (**1N**), Zr (**2N**), and Hf (**3N**)). Hydrogen atoms omitted for sake of clarity.

Table 1 together with the related experimental data where available.[31,70]

Table 1. Main geometrical parameters optimized for the Group 4 complexes $[M(bp)_3]^{2-}$ (**1P–3P**) and $[M(bpy)_3]^{2-}$ (**1N–3N**) for M = Ti, Zr, and Hf, respectively. M–P(N) is the average metal–ligand distance, and C–C and C=P(N) are the distances in the central unit of the bp (bpy) ligands. In parentheses are given the available experimental data taken from references [31,70]. Bond lengths in angstroms and angles in degrees.

Complex	M	L–L	θ	M–P(N)	C–C	C=P(N)
1P	Ti	bp	0.0 (0.0)	2.438 (2.400)	1.447 (1.44)	1.815 (1.768)
2P	Zr	bp	0.0 (3.0)	2.606 (2.544)	1.444 (1.434)	1.818 (1.780)
3P	Hf	bp	0.0 (0.0)	2.573 (2.517)	1.440 (1.413)	1.818 (1.777)
1N	Ti	bpy	43.8	2.110	1.398	1.429
2N	Zr	bpy	36.7 (33.4)	2.257 (2.213)	1.398 (1.36)	1.438 (1.435)
3N	Hf	bpy	37.3	2.218	1.391	1.442

Metal–ligand bond lengths are overestimated by 0.039–0.062 Å, a range of deviations usually found at this level of theory.[71] Note that the evolution of the experimental M–P distances on going from **1P** to **2P** (increase) and from **2P** to **3P** (decrease) is properly reproduced by these calculations. Smaller deviations were found for the bond lengths associated with the central unit of the chelate ligands, with overestimations between 0.003 and 0.047 Å. In agreement with the experimental data, an ideal TP structure ($\theta = 0°$) was found for tris-biphosphinine complexes **1P–3P**. In marked contrast, the structures optimized for the tris-bipyridine complexes exhibit theoretical θ angles of 43.8, 36.7 (exptl 33.4), and 37.3° for **1N**, **2N**, and **3N**, respectively. Taking into account the values of the bpy bite angles (75.7, 71.5 and 72.8°, respectively), these structures are not far from those expected for the OC limit[56] ($\theta = 43.1$, 38.0, and 39.5°, respectively). Therefore, depending on the nature of the chelate ligand, either the TP structure (L–L = bp) or a nearly OC structure (L–L = bpy) was found in the family of Group 4 $[M(L–L)_3]^{2-}$ transition-metal complexes.

Another interesting feature of these structures is the geometrical changes induced in the ligands on coordination. For sake of comparison, the bridging C–C and internal C=P(N) bond lengths optimized in the (N)P=C–C=P(N) central unit of the neutral, monoanionic, and dianionic isolated bp (bpy) ligands are reported in Table 2. It appears that adding one or two electrons to the isolated ligand entails shortening of the C–C bridge between the two phosphinine (pyridine) subunits and lengthening of the C=P(N) bonds. Both these trends are consistent with the shape of the LUMO of the neutral species (Scheme 1), which is C–C bonding and C=P(N) antibonding.[72] Now if one considers the geometry of the coordinated ligands (Table 1), it is clear that there is shortening of the C–C bond and lengthening of the C=P(N) bonds with respect to the values optimized in the isolated neutral ligands (Table 2). These distortions suggest pronounced electron delocalization from the metal center into the lowest π* orbitals of the chelate ligands, a result consistent with the MO analysis of the d–π* interactions above.

Table 2. Bridging C–C and internal C=P(N) bond lengths optimized for the central unit of the isolated biphosphinine (bp) and bipyridine (bpy) ligands (neutral, monoanionic, and dianionic) in the *cis* arrangement depicted in Scheme 1. Bond lengths in angstroms.

	bp	$bp^{\bullet-}$	bp^{2-}	bpy	$bpy^{\bullet-}$	bpy^{2-}
C–C	1.506	1.455	1.415	1.498	1.442	1.400
C=P(N)	1.782	1.832	1.891	1.351	1.394	1.444

A more detailed analysis, however, reveals that bp and bpy ligands accommodate this release of electron density from the metal in different ways. For instance, consider the C–C and C=P(N) distances in the bp (bpy) ligands of zirconium complex **2P** (**2N**). The optimized values in **2P** (1.444 and 1.818 Å for C–C and C=P, respectively) are close to those optimized in the isolated monoanionic bp ligand (1.455 and 1.832 Å, respectively). On the other hand, the values optimized for C–C and C=N in **2N** (1.395 and 1.438 Å, respectively) are close to those optimized in the isolated dianionic bpy ligand (1.400 and 1.444 Å, respectively). It is noteworthy that this result is in nice agreement with the experimental structure of $[Zr(bpy)_3]^{2-}$ and $[Zr(bp)_3]^{2-}$.[31] According to these geometrical observations (which also hold for titanium and hafnium complexes), complexes **1N–3N** can be roughly described as the coordination of three bipyridine dianions to an M^{IV} metal center, while in complexes **1P–3P** the electron density is shared between metal and ligands. In the next section we show that this different behavior can be traced to a change in the electronic configuration of the complex.

*Electronic structure of the **1P–3P** and **1N–3N** minima*: The TP complexes **1P–3P** were found to be nearly of C_{3h} symmetry, so their electronic structure was analyzed in this symmetry group. The three low-lying d orbitals, occupied according to the formal d^6 electron count, transform as a′ + e′, and the same holds for the three symmetry-adapted orbitals built from the π* LUMO of each bp ligand [quoted in the following as π*(a′) and π*(e′)]. Thus, on symmetry grounds, there is the possibility to stabilize the three d levels by bonding interactions with the three lowest lying π* orbitals on the ligands.

Let us consider, for example, the electronic structure of zirconium bp complex **2P**. The shape of the three highest occupied (HO) and the lowest unoccupied (LU) molecular orbitals are shown in Figure 2a. The HOMO−1 constitute the set of degenerate e′ MOs which exhibit d–π* bonding interactions, as expected from the Hoffmann analysis and from the symmetry properties described above. However, decomposition of these orbitals into their metal and ligand components shows that they are mainly developed on the ligands (75.1% instead of 24.9% on the metal), mostly through the contribution of the low-lying π*(e′) orbitals (63.0%). The

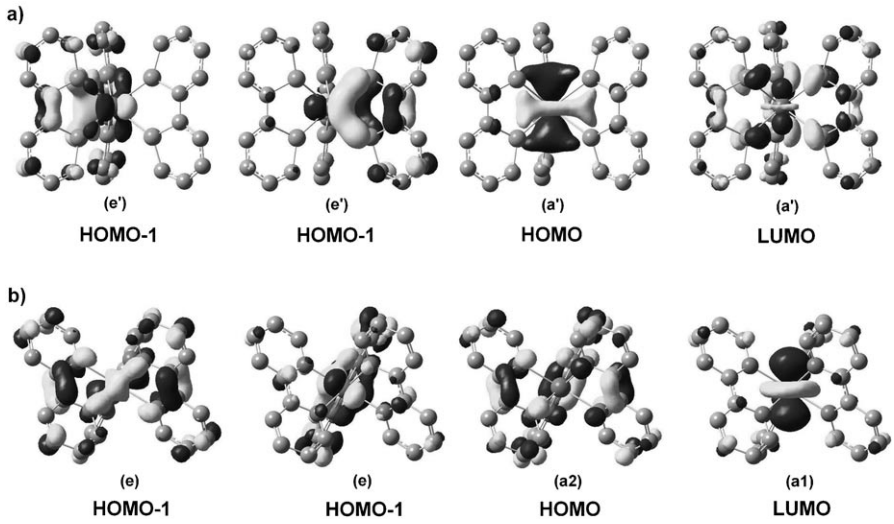

Figure 2. Drawings of the HOMO−1, HOMO, and LUMO of a) **2P** with symmetry labels according to C_{3h} symmetry; b) **2N**, with symmetry labels according to D_3 symmetry. Hydrogen atoms omitted for sake of clarity.

stabilization energy arising from the d–π* bonding interactions is evidenced by the energy level of these two MOs. While they were predicted on the basis of σ interactions (Scheme 3) to be the highest occupied orbitals in a d^6 TP structure, they actually prove to be the HOMO−1 in zirconium complex **2P**. On the other hand, the HOMO (a′) is a metal-centered orbital (53.5%, mainly z^2) stabilized by bonding interactions with two ligand orbitals: 1) the third low-lying π*(a′) orbital (25.7%);[73] and 2) the a′ combination of a ligand orbital, which is mainly of σ*(P=C) character (19.2%). As can be seen in **1**, the shape of this orbital perfectly matches that of z^2 in the TP geometry. Finally, the LUMO is a ligand-centered orbital (88.6%), mainly formed by π*(a′) (71.1%) in antibonding interaction with z^2 (11.4%). In conclusion, the large ligand contributions in the three highest occupied MOs clearly show that the usual d^6 electron count (three neutral bp ligands) in **2P** is purely formal. On the other hand, due to the significant metal contribution in the HOMO, the d^0 limit (three dianionic bp ligands) is also not appropriate. According to the metal/ligand percentages given above for the three highest occupied MOs, 2.1 electrons can be attributed to the metal and 3.9 to the ligands, of which 3.0 are in the three low-lying π* ligand orbitals.[74] This result is consistent with the experimental[31] and theoretical structural data (Tables 1 and 2), since the geometry of the coordinated bp ligand is close to that of the isolated monoanionic species. Note that the same MO analysis and conclusions hold for the titanium and hafnium complexes (**1P** and **3P**).

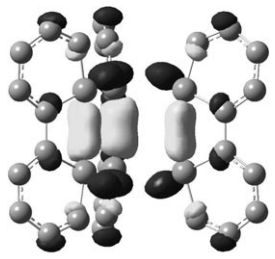

1

Let us now describe the electronic structure of the nitrogen analogue, $[Zr(bpy)_3]^{2-}$ (**2N**), for which theoretical and experimental structures ($\theta = 36.7$ and 33.4°, respectively) are close to the octahedral limit. The optimized structure is of nearly D_3 symmetry, so the labels used in the following are those of that symmetry group. The three low-lying d orbitals transform as $a_1 + e$, and the π* LUMOs on the bpy ligands as $a_2 + e$. Therefore, in this complex, only two of the three d orbitals can be stabilized by bonding interactions with the lowest lying π* ligand orbitals (the set of degenerate e MOs). The shape of the three highest occupied orbitals and that of the lowest vacant orbital of complex **2N** are given in Figure 2b. As was found for the phosphorus analogue **2P**, the HOMO−1 constitute a set of degenerate e MOs mostly developed on the ligands (82.3%). The delocalization toward the π*(e) orbitals is even greater than in **2P** (69.3 instead of 63.0%), while the contribution on the metal is smaller (17.7 instead of 24.9%). The greatest change, however, occurs in the HOMO, which is entirely localized on the ligands and formed by the low-lying π*(a_2) orbital (93.7%). In contrast, the LUMO (a_1) is a metal-centered orbital (58.5%, mainly z^2) stabilized by a π*(a_1) orbital (32.5%), depicted in **2**. Therefore, compared to the phosphorus analogue **2P**, there is an inversion in the localization of the frontier orbitals: in **2N** the HOMO is ligand-centered and the LUMO metal-centered, while the opposite is true for **2P**.

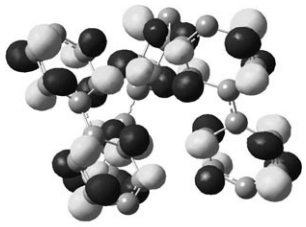

2

On the whole, the three highest occupied MOs ($e + a_2$) of **2N** are mostly (e) or entirely (a_2) developed on the bpy ligands. According to the metal/ligands percentages given above for the three highest occupied MOs, 0.7 electrons can be attributed to the metal and 5.3 to the ligands (of which 4.7 are in the three low-lying π* ligand orbitals), so that the electronic configuration of this formal d^6 complex is actually close to d^0 with a Zr^{IV} center in interaction with three dianionic ligands. This result accounts for the experimental[31] and theoretical structural data (Tables 1 and 2), since the geometry of the coordinated bpy ligand was found to be close to that of the isolated dianionic species. Comparison of the shape of the three highest occupied MOs in **2P** and **2N** shows that the main reason why bp and bpy ligands accommodate the release of electron density from the metal in different ways is the change in the localization of the HOMO, which is a pure ligand orbital [π*(a_2)] in **2N** and a mainly metal-centered orbital (z^2) in **2P**. This change in electronic

structure between bp and bpy complexes was also found for the Ti (**1P** and **1N**) and Hf (**3P** and **3N**) analogues.

However, bp and bpy complexes do not differ only in their electronic structure but also in their geometry. At this stage, it is difficult to rationalize why bp complexes adopt a TP geometry while their bpy analogues, with a nearly d^0 configuration, are close to the OC limit. To analyze the factors responsible for this structural change, the potential energy curves and the MO correlation diagrams connecting the OC and TP limits were computed for the six complexes (M = Ti, Zr, Hf and L-L = bp, bpy).

Octahedron→trigonal prism potential energy curves and MO correlation diagrams: In these calculations, the potential-energy curve connecting the OC and TP structures was studied for each complex. The geometry of the complex was optimized for several values of θ between 50 and 0°. The shape of the energy curve $E(\theta)$ was analyzed with the help of the correlation diagram drawn for the three highest occupied MOs of these formally d^6 complexes.

The results found for the three bp complexes (M = Ti, Zr, Hf) were similar for both the potential-energy curve and the MO correlation diagram. The energy curves $E(\theta)$ exhibit a single minimum for $\theta = 0°$ (Figure 3), that is, the TP structures **1P**–**3P** characterized as minima in the previous section. Let us now consider the MO correlation diagram associated with this OC→TP distortion for zirconium complex **2P** (Figure 4). The degenerate orbitals HOMO−1, which were expected to be destabilized on the basis of σ interactions only (Scheme 3), were found to be slightly stabilized (by less than 2 kcal mol^{-1}) by this distortion: the participation of the degenerate low-lying π* orbitals increases from 59 to 63%. The most striking feature of this correlation diagram, however, is the energetic evolution of the HOMO (mainly z^2). While it was expected to remain unperturbed (Scheme 3), Figure 4 reveals that it is actually significantly stabilized (by 13.4 kcal mol between $\theta = 50$ and 0°), so that the HOMO should play a crucial role in stabilizing the TP structure.

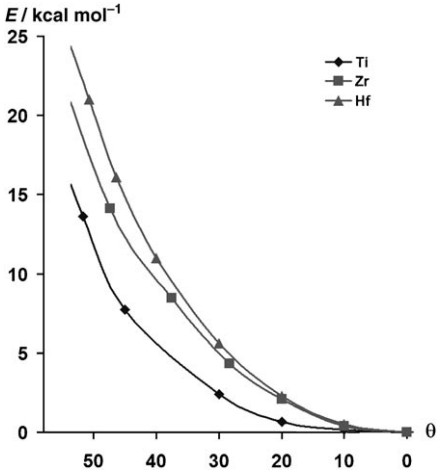

Figure 3. Potential-energy curves calculated as a function of trigonal twist angle θ (defined in Scheme 4) for the $[M(bp)_3]^{2-}$ complexes (M = Ti, Zr, and Hf).

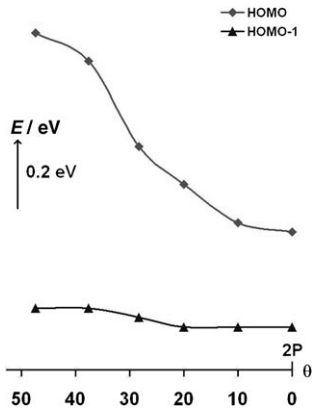

Figure 4. Orbital correlation diagram for the three highest occupied MOs of $[Zr(bp)_3]^{2-}$ as a function of the trigonal twist angle θ.

This unexpected result was analyzed by examining how the stabilizing participation of the vacant ligand orbitals to the HOMO varies as a function of θ. For $\theta = 50°$, z^2 is stabilized by interaction with the phosphorus analogue of the π* orbital pictured in **2** (the same was found for the LUMO of the nearly octahedral bpy analogue **2N**). Its participation (34%) decreases with decreasing θ and eventually vanishes in the TP structure. At the same time, the contribution of the non-degenerate low-lying π* ligand orbital increases from 0 to 25.7%. These two factors should more or less cancel each other. Finally, the σ*(P=C) component **1** increases from 5 to 19%, a trend which contributes to stabilization of the HOMO in the TP structure.[75] On the whole, the energetic evolution of the three highest occupied MOs, and in particular that of the HOMO, is consistent with the TP structure found for bp complexes (similar correlation diagrams were found for the Ti and Hf bp complexes). However, it is important to recall that repulsion between ligands is known to disfavor the TP structure and thus to work against the electronic factors described above. By using the geometries optimized for the various values of θ, this repulsion energy was computed by removing the metal center and assuming the bp ligands to be monoanionic in order to take into account the repartition of the electron density in the whole complex. In complexes **1P**–**3P**, the smallest repulsion energy was found for $\theta = 37.0$, 32.0, and 34.0°, respectively, values which are actually very close to those predicted for the OC structure (39.0, 35.3, and 35.9°, respectively).[56] These results confirm that minimization of repulsion between the ligands is achieved for a pseudo-octahedral arrangement. However, this factor is not large enough in Group 4 $[M(bp)_3]^{2-}$ complexes to overcome the electronic factors favoring the TP structure, as shown by the total-energy curves reported in Figure 3.

The importance of the energetic evolution of the HOMO in fixing the TP geometry of zirconium complex **2P** was also evidenced by studying the geometrical consequences of its oxidation. According to our analysis, removing one electron from the HOMO should decrease the preference for the TP structure. This prediction is in nice agreement with the experimental structure of the monoanionic complex $[Zr(bp)_3]^-$ ($\theta = 21$–$24°$)[70] and with its optimized theoretical structure ($\theta = 19.7°$). This trend is strengthened if one considers the as-yet unknown neutral complex $[Zr(bp)_3]$, which is predicted to adopt an OC geometry ($\theta = 45.9°$) despite the fact that the degenerate orbitals of mainly ligand π* character are still fully occupied.

Similar calculations were performed for the three bpy complexes by optimizing the geometry of the complex for each value of θ. Surprisingly, each potential energy curve $E(\theta)$ exhibits two minima (Figure 5): an absolute minimum (**1N**–**3N**, Figure 1) and a secondary minimum with a TP geometry of nearly C_{3h} symmetry (**1N′**–**3N′**, Figure 6 and Table 3).

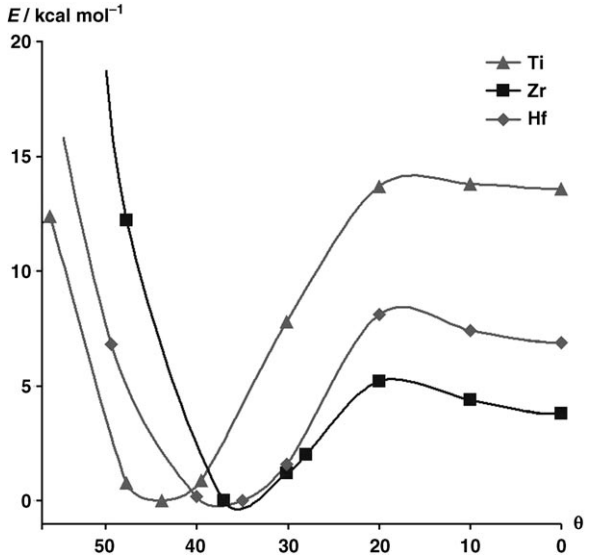

Figure 5. Potential-energy curves calculated as a function of trigonal twist angle θ (defined in Scheme 4) for the $[M(bpy)_3]^{2-}$ complexes (M = Ti, Zr, and Hf).

Figure 6. Optimized structures of the $[M(bpy)_3]^{2-}$ complexes in their secondary minima of TP geometry (M = Ti (**1N′**), Zr (**2N′**), and Hf (**3N′**)). Hydrogen atoms omitted for sake of clarity.

The energy difference between the two minima increases in the order: Zr (+3.8) < Hf (+6.9) < Ti (+13.6 kcal mol^{-1}).[76] In the zirconium secondary minimum **2N′**, the three highest occupied MOs are still mostly located on the ligands: 89.4% in the set of degenerate orbitals HOMO−1 and 82.0% in the HOMO. It is noteworthy that, while the σ*(P=C) orbital **1** has been shown to stabilize the HOMO of TP complexes **1P**–**3P**, no participation of the analogous nitrogen σ*(N=C) orbital is found in the HOMO of **1N′**–**3N′**. This difference can be traced to the energy level of this σ* orbital, which is located 7.7 eV higher in energy in the bpy than in the bp ligand. According to the percentages given above, only 0.8 electrons of this formally d^6 complex can be attributed to the metal center. Therefore, **2N′** can be described approximately as three dianionic bpy ligands in interaction with a Zr^{IV} metal center. This conclusion is also evidenced by the C−N and C−C bond lengths optimized in the complex, which are close to those optimized in the isolated bpy^{2-} dianionic ligand (Tables 2 and 3). Similar results were found for the Ti and Hf complexes (**1N′** and **3N′**, respectively).

Table 3. Main geometrical parameters optimized for the $[M(bpy)_3]^{2-}$ secondary minima **1N′**–**3N′** for M = Ti, Zr, and Hf, respectively. M−N is the metal–ligand distance, and C−C and C=N are the distances in the central unit of the bpy ligands. Bond lengths in angstroms and angles in degrees.

Complex	M	L–L	θ	M−N	C−C	C=N
1N′	Ti	bpy	0.0	2.135	1.395	1.429
2N′	Zr	bpy	0.0	2.266	1.393	1.437
3N′	Hf	bpy	0.0	2.229	1.389	1.440

The main electronic reorganization between **2N** and **2N′** concerns the HOMO. It was the pure π*(a_2) orbital in **2N** (nearly D_3 symmetry) whereas a bonding interaction can develop between π*(a′) and z^2 in **2N′** (nearly C_{3h} symmetry). As shown by the correlation diagram in Figure 7, the HOMO is actually stabilized for small values of θ. Taken alone, the energetic evolution of the HOMO would favor the secondary minimum **2N′**. At the same time, however, the set of degenerate orbitals is destabilized (by 2.6 kcal mol^{-1}), a factor which works in favor of the absolute

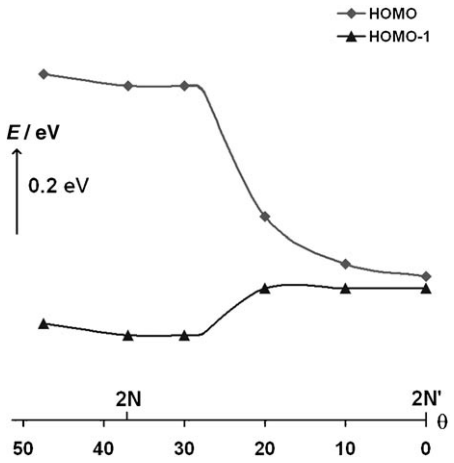

Figure 7. Orbital correlation diagram for the three highest occupied MOs of $[Zr(bpy)_3]^{2-}$ as a function of the trigonal twist angle θ.

minimum **2N**. On the basis of this correlation diagram, one gets a qualitative understanding of the possible existence of two minima for the bpy complex, but the trigonal prism seems to be favored. On the other hand, the evolution of the energy difference ($\Delta E_{\mathbf{N}\rightarrow\mathbf{N}'}$) as a function of the metal center cannot be rationalized on the basis of this diagram. For instance, the HOMO is slightly more stabilized for Ti than for Zr (12.1 instead of 9.8 kcal mol^{-1}), and the degenerate HOMO−1 slightly less destabilized (1.9 instead of 2.6 kcal mol^{-1}). One would then conclude that $\Delta E_{\mathbf{N}\rightarrow\mathbf{N}'}$ decreases on going from Ti to Zr, while it actually increases from 3.8 to 13.6 kcal mol^{-1}.

To rationalize these results, a thermodynamic cycle connecting the two minima **N** and **N′** was constructed in the following way (Scheme 5). The absolute minimum of type **N**,

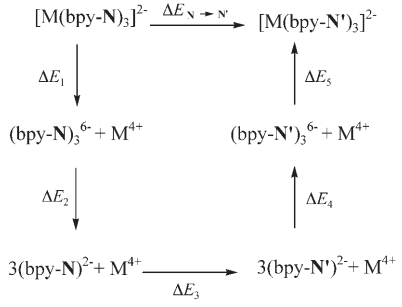

Scheme 5.

denoted $[M(bpy\text{-}\mathbf{N})_3]^{2-}$, is first decomposed into an M^{4+} metal center and the set of three dianionic ligands $(bpy\text{-}\mathbf{N})_3^{6-}$ while their geometries in the starting complex are kept unchanged (ΔE_1); then the three ligands are separated ($\rightarrow 3\,(bpy\text{-}\mathbf{N})^{2-}$) without any change in their internal structure (ΔE_2); the internal geometry of the three isolated ligands is then reorganized ($\rightarrow 3\,(bpy\text{-}\mathbf{N}')^{2-}$) to that actually found in the secondary minimum **N′** (ΔE_3); the three ligands are put together ($\rightarrow (bpy\text{-}\mathbf{N}')_3^{6-}$) in the geometry they have in **N′** (ΔE_4); finally, the TP complex **N′** is formed ($[M(bpy\text{-}\mathbf{N}')_3]^{2-}$) by adding the M^{4+} metal center to the set of three dianionic ligands (ΔE_5). By using this thermodynamic cycle, the energy difference between the two minima ($\Delta E_{\mathbf{N}\rightarrow\mathbf{N}'}$) can thus be decomposed into a series of three terms with a clear physical meaning: 1) $\Delta E_1+\Delta E_5$ is the energetic change in the metal–ligands interaction on going from **N** to **N′**; 2) $\Delta E_2+\Delta E_4$ is the change in ligand–ligand repulsion; 3) ΔE_3 is the energy variation associated with reorganization of the internal geometry of the ligands.

The results of these calculations are reported in Table 4. The term $\Delta E_1+\Delta E_5$ is negative for all three complexes, which means that the metal–ligands interaction is more stabilizing in the secondary minimum **N′** than in the absolute minimum **N.** Therefore, it cannot rationalize the energetic ordering of the two minima. However, it contributes to the evolution of $\Delta E_{\mathbf{N}\rightarrow\mathbf{N}'}$ as a function of the metal center (Zr < Hf < Ti), since the stabilization energy increases (in absolute value) in the order Zr > Hf > Ti. The term $\Delta E_2+\Delta E_4$ is positive whatever the metal center. As expected, ligand–ligand repulsion is larger in the TP secondary minimum **N′** and thus favors the absolute minima **N** of pseudo-octahedral geometry. Interestingly, this repulsion (between 7.4 and 8.0 kcal mol^{-1}) is almost independent of M and thus does not contribute to the large variations found in $\Delta E_{\mathbf{N}\rightarrow\mathbf{N}'}$ as a function of the metal center. Finally, the last term of the thermodynamic cycle (ΔE_3) makes **N′** definitely less stable than **N** since it is large and positive for the three metal centers. Furthermore its evolution (12.4, 6.6, and 8.4 kcal mol^{-1} for M = Ti, Zr, and Hf, respectively) parallels that of $\Delta E_{\mathbf{N}\rightarrow\mathbf{N}'}$: Zr < Hf < Ti. Therefore, the internal distortion energy of the bpy ligands on going from **N** to **N′** contributes significantly to the evolution of the energy difference between the two minima as a function of the metal center. In conclusion, this energy decomposition showed the metal–ligands interaction to be more favorable in the TP secondary minima **N′**. However, both ligand–ligand repulsion and internal distortion energy of the ligands make pseudo-octahedral structures of type **N** the absolute minima for the Group 4 $[M(bpy)_3]^{2-}$ complexes.

Table 4. Energy decomposition [kcal mol^{-1}] of the energy difference $\Delta E_{\mathbf{N}\rightarrow\mathbf{N}'}$ between the two minima **N** (pseudo-OC) and **N′** (TP) in $[M(bpy)_3]^{2-}$ complexes (M = Ti, Zr, and Hf), according to the thermodynamic cycle given in Scheme 5.

	1N→1N′ (Ti)	**2N→2N′** (Zr)	**3N→3N′** (Hf)
$\Delta E_1+\Delta E_5$	−6.8	−10.4	−8.9
$\Delta E_2+\Delta E_4$	+8.0	+7.6	+7.4
ΔE_3	+12.4	+6.6	+8.4
$\Delta E_{\mathbf{N}\rightarrow\mathbf{N}'}$	**+13.6**	**+3.8**	**+6.9**

Group 6 $[M(bp)_3]$ complexes and comparison with Group 4

Geometrical structure of the minima: In this section, we exclusively focus on two neutral Group 6 tris-biphosphinine complexes $[M(bp)_3]$ with M = Mo and W. All the complexes of the triad have been synthesized, but only the structure of the tungsten complex has been experimentally determined.[32] In particular the sensitivity of the chromium complex precluded determination of an X-ray crystal structure. The optimized structures for $[M(bp)_3]$ neutral complexes **4P** and **5P** (M = Mo and W, respectively) are shown in Figure 8; the main theoretical parameters are reported in Table 5.

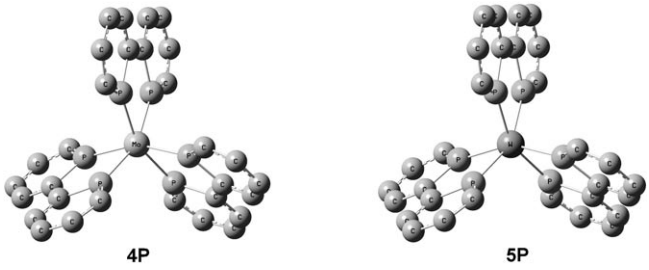

Figure 8. Optimized geometries of $[M(bp)_3]$ complexes (M = Mo (**4P**), W (**5P**)). Hydrogen atoms omitted for clarity.

Table 5. Main geometrical parameters optimized for the Group 6 complexes $[M(bp)_3]$ (**4P** and **5P**) for M = Mo and W, respectively. M–P is the average metal–ligand distance, and C–C and C=P are the distances in the central unit of the bp ligands. In parentheses are given the available experimental data taken from reference [32]. Bond lengths in angstroms and angles in degrees.

Complex	M	L–L	θ	M–P	C–C	C=P
4P	Mo	bp	32.9	2.420	1.468	1.779
5P	W	bp	29.7 (15.0)	2.411 (2.360)	1.463 (1.444)	1.778 (1.742)

The major change with respect to Group 4 biphosphinine complexes concerns their overall geometry. The equilibrium θ values (32.9 and 29.7° for M = Mo and W, respectively) were found to be intermediate between the TP ($\theta = 0°$) and OC ($\theta = 42.2°$ for a bite angle of 75°)[56] limits, whereas their Group 4 analogues are trigonal-prismatic. This trend is in agreement with the available experimental data[31,32] for the third transition series, since $\theta = 15°$ for M = W (**5P**) instead of 0° for M = Hf (**3P**). On the other hand, ligand reorganization on complexation also differs on going from **3P** to **5P**: the C–C internal bond length increases by 0.028 Å, while the internal C=P bond length decreases by 0.040 Å, in nice agreement with the experimental trends (Δ(C–C) = +0.031 Å and Δ(C=P) = −0.035 Å, Tables 1 and 5). The geometry of the bp ligands in **5P** can thus be roughly described as intermediate between those of the neutral and monoanionic isolated species, a result which suggests that electron transfer from the metal center to the low-lying ligand π* orbitals decreases on going from Group 4 dianionic to Group 6 neutral bp complexes.

*Electronic structure of the minima (**4P**, **5P**)*: Complexes **4P** and **5P** were found to be nearly of D_3 symmetry, so their electronic structure will be analyzed within this symmetry group. Consider, for example, the electronic structure of the tungsten complex **5P**. The shapes of the three highest occupied (HO) and the lowest unoccupied molecular orbitals (LUMO) are shown in Figure 9. The energy ordering of the

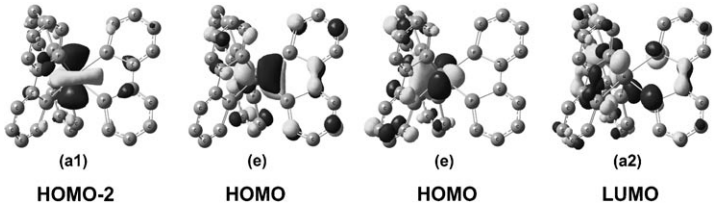

Figure 9. Drawings of the HOMO−2, HOMO, and LUMO of **5P** with symmetry labels according to D_3 symmetry. Hydrogen atoms omitted for clarity.

occupied orbitals differs from that found for the Group 4 complexes, since the HOMO is now made up of the set of degenerate e orbitals, and the nondegenerate orbital of a_1 symmetry is the HOMO−2. In the set of e MOs, the metal contribution is equal to 35.7% while the ligand contribution can be divided into two main terms: 1) a stabilizing bonding interaction with the low-lying π*(e) vacant orbitals (31.7%), that is, a percentage significantly smaller than that found in the Group 4 complexes (63% in **2P**, for instance); 2) a destabilizing antibonding interaction with two sets of degenerate occupied ligand orbitals (21.1% instead of only 2.4% in **2P**).[77] Therefore, the contribution of π* (π) orbitals in the set of degenerate MOs is smaller (larger) in **5P** than in **2P**, trends that can be traced to the lowering of d levels on going from a dianionic (Group 4) to a neutral (Group 6) complex. The nondegenerate HOMO−2 has a metal contribution of 48.1% (mainly z^2) and again exhibits two kind of interactions with the ligand orbitals: 1) weak bonding interactions with the σ*(P=C) (8.1%) and π*(a_1) (6.4%) vacant orbitals (**1** and the bp analogue of **2**, respectively); 2) an antibonding interaction with an occupied a_1 combination of π bonding orbital on the ligands (30%), whereby the bonding combination is located just below the d-block orbitals (HOMO−3). Finally, the LUMO is a purely ligand orbital (98.5%), almost entirely developed on the third low-lying π*(a_2) ligand orbital. On the whole, the contribution of the three low-lying π* orbitals in the three highest occupied MOs of complex **5P** is significantly smaller than in Group 4 complexes **1P**–**3P**. According to the percentages given above, only 1.4 electrons can be attributed to these low-lying π* ligand orbitals in **5P** instead of 3.0 for **2P**, a result in agreement with the evolution of the ligands' geometry described in the previous section: nearly monoanionic geometry of the bp ligands in **2P** and intermediate between monoanionic and neutral geometries in **5P**. Similar analysis and conclusions hold for the molybdenum complex **4P**.

Octahedron→trigonal prism potential-energy curves and MO correlation diagrams: In these calculations, the geometry of complexes **4P** and **5P** was optimized for several values of the θ between 50 and 0°; the potential-energy curves are shown in Figure 10. Similar results were found for the two complexes and only tungsten complex **5P** is considered in the following.

The energy curve $E(\theta)$ exhibits a single minimum for $\theta =$ 29.7°, that is, the structure characterized above as a minimum (**5P**). On the other hand, the TP structure ($\theta = 0°$) was characterized as a transition state of nearly D_{3h} symmetry. Let us now focus on the MO correlation diagram between these two stationary points (**5P**→TP ($\theta = 0°$), Figure 11). The energy of the degenerate orbitals is almost constant (stabilization of 1.4 kcal mol^{-1}). The stabilizing participation of the degenerate low-lying π* orbitals increases from 31.7 to 37.9%, while the destabilizing contribution of occupied ligand orbitals increases from 21.1 to 23.0%. The largest energy variation is, however, found in the nondegenerate HOMO−2, which is stabilized by 16.6 kcal mol^{-1}. In this orbital (mainly z^2), the small π*(a_1) contribution found in the D_3 minimum (6.4%) vanishes in the TP structure because

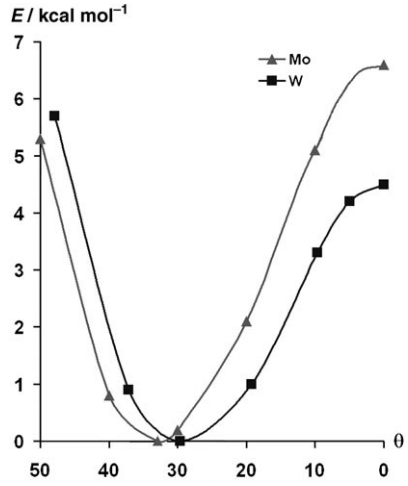

Figure 10. Potential-energy curves calculated as a function of trigonal twist angle θ (defined in Scheme 4) for the $[M(bp)_3]$ complexes (M = Mo, W).

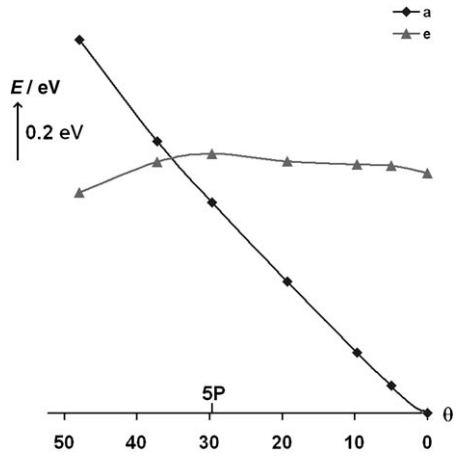

Figure 11. Orbital correlation diagram for the three highest occupied MOs of the $[W(bp)_3]$ complex as a function of trigonal twist angle θ.

the z^2 and π^* components become of different symmetry in the nearly D_{3h} TP structure (a'_1 and a_1'', respectively). The two other ligand contributions, however, contribute to the large stabilization found for HOMO−2: 1) the stabilizing participation of σ*(P=C) increases from 8.1 to 21.6%; 2) the destabilizing participation of $\pi(a_1)$ occupied ligands orbital (30% in the D_3 minimum) vanishes by symmetry in the nearly D_{3h} TP structure (a_1' and a_1'' for z^2 and π components, respectively). At the same time, the bonding combination of $\pi(a_1)$ and z^2 is destabilized (HOMO−3, not shown in Figure 11), but on the whole the relief of the $z^2 \rightarrow \pi(a_1)$ two-orbital four-electron interaction favors the TP structure.

It is thus clear that the minimum-energy structure found for the tungsten complex (**5P**, $\theta = 29.7°$) cannot be rationalized by the correlation diagram on Figure 11, which would lead to prediction of a TP structure. To understand the factors which disfavor the TP structure and the change of geometry between **2P** ($\theta = 0°$) and **5P** ($\theta = 29.7°$), we made use of a thermodynamic cycle similar to that depicted in Scheme 5. However, to take into account the repartition of the electronic density in the whole complexes, the dissociated bp ligands were assumed to be monoanionic for the zirconium complex **2P**, and two sets of calculations were performed for tungsten complex **5P**, assuming either monoanionic or neutral dissociated ligands. The limit structures used for **5P** in the cycle were $\theta = 29.7°$ (minimum) and 0° (TP), and their energy difference ΔE was $+4.5$ kcal mol^{-1}. Similar calculations were performed for **2P** structures with $\theta = 30$ and 0° (TP, minimum), whose energy difference ΔE is -4.5 kcal mol^{-1}.

The results of the energy decomposition (Table 6) afford answers to the two questions addressed above. The stabilizing metal–ligand interaction is larger in the TP structure

Table 6. Energy decomposition [kcal mol^{-1}] of the energy difference ΔE according to a thermodynamic cycle similar to that depicted in Scheme 5. For the tungsten complex $[W(bp)_3]$, the cycle is constructed between the structures with $\theta = 29.7°$ (minimum-energy structure **5P**) and $\theta = 0°$ (TP structure), with dissociated ligands either monoanionic or neutral (values in parentheses). For the zirconium complex $[Zr(bp)_3]^{2-}$, the cycle is constructed between the structures with $\theta = 30°$ and $\theta = 0°$ (minimum-energy TP structure, **2P**) with monoanionic dissociated ligands.

	5P (29.7°, min.)→**5P** (0°)	**2P** (30°)→**2P** (0°, min.)
$\Delta E_1 + \Delta E_5$	−5.4 (−8.8)	−8.8
$\Delta E_2 + \Delta E_4$	+9.7 (+10.3)	+3.2
ΔE_3	+0.2 (+3.0)	+1.1
ΔE	+4.5	−4.5

($\Delta E_1 + \Delta E_5 < 0$), by 8.8 kcal mol^{-1} in **2P** and 7.1 kcal mol^{-1} in **5P** (mean value). According to this factor alone, a TP structure would be expected for both complexes. On the other hand, the TP structure is disfavored by the increased ligand–ligand repulsion ($\Delta E_2 + \Delta E_4$). This term is significantly larger for tungsten complex **5P** (av +10.0 kcal mol^{-1}) than for zirconium complex **2P** (+3.2 kcal mol^{-1}). Finally, the change in the internal distortion energy (ΔE_3) of the ligands (av +1.6 kcal mol^{-1} in **5P** and +1.1 kcal mol^{-1} in **2P**) is small and similar in both complexes. According to this energy decomposition, the structural change between **2P** (TP) and **5P** (intermediate between the OC and TP limits) can be mainly traced to the increased repulsion between the ligands in the TP structure, which is 7 kcal mol^{-1} larger in the tungsten than in the zirconium complex. A possible explanation for this trend might be the evolution of the ligand–ligand distances in the TP geometry. The optimized M−P bond lengths are shorter for M = W than for M = Zr, by about 0.2 Å (2.416 vs 2.606 Å). The same holds for the closest P···P distance involving two bp ligands (3.342 and 3.708 Å for M = W and Zr, respectively). It is thus conceivable that tungsten complex **5P** evolves toward a structure intermediate between the TP and OC limits to relieve the ligand–ligand repulsion in the TP structure. Such a relationship between metal–ligand distance and equilibrium twist angle was already suggested by Holm et al. for a series of tris-diimine complexes.[78]

Conclusion

In agreement with the available experimental data, DFT calculations led to a trigonal prismatic (TP) structure for Group 4 tris-biphosphinine complexes $[M(bp)_3]^{2-}$ (**1P**–**3P**) and to a nearly octahedral (OC) structure for their tris-bipyridine analogues $[M(bpy)_3]^{2-}$ (**1N**–**3N**) (M = Ti, Zr, and Hf). A secondary minimum of TP structure (**1N′**–**3N′**) was, however, located for the bpy complexes. By use of a thermodynamic cycle connecting the two minima, the TP structures (**N′**) were found to be disfavored with respect to the pseudo-OC ones (**N**) owing to larger ligand–ligand repulsion and internal distortion energy of the ligands. While the formal electronic configuration of these complexes is d^6, the degenerate molecular orbitals HOMO−1 of bp and bpy complexes are mainly developed on the degenerate low-lying π* ligand orbitals. However, the electronic structure of the complexes differs by the HOMO composition, which is mainly metal-centered in bp complexes and consists of the pure third low-lying π* ligand orbital in bpy complexes. Therefore, $[M(bp)_3]^{2-}$ and $[M(bpy)_3]^{2-}$ complexes differ by the way in which the ligands accommodate the release of electron density from the metal center. $[M(bpy)_3]^{2-}$ complexes can be approximately described as the coordination of three bipyridine dianions to a d^0 center. The electron density is more delocalized between the metal and the ligands in $[M(bp)_3]^{2-}$ complexes, and the geometry of the coordinated ligands is close to that found for the isolated bp monoanion. Finally, the energetic evolution of the HOMO between the OC and TP limit structures allows a simple rationalization of the geometrical changes found on oxidation of the $[Zr(bp)_3]^{2-}$ complex (TP, intermediate, and OC structures for the dianionic, monoanionic, and neutral complex, respectively).

In Group 6 $[M(bp)_3]$ neutral complexes (**4P** and **5P** for M = Mo and W, respectively), the DFT equilibrium geometries were found to be intermediate between the OC and TP limits, in agreement with available experimental data, while the TP structures were characterized as transition states. Electron transfer from the metal to the π* ligand orbitals is significantly smaller than in their Group 4 dianionic analogues (**1P**–**3P**), and the geometry of the coordinated ligands is intermediate between those of the isolated monoanionic and neutral bp ligands. The change of the experimental structure between $[Zr(bp)_3]^{2-}$ (**2P**, TP) and $[W(bp)_3]$ (**5P**, intermediate between TP and OC limits) was rationalized by use of a thermodynamic cycle and mainly traced to the increased ligand–ligand repulsion in the TP structure. It is larger in the tungsten than in the zirconium complex, a trend which correlates with the evolution of the metal–ligand distances (W–P < Zr–P).

Acknowledgements

We thank the CNRS, the Ecole Polytechnique, and the Université Paris-Sud (Orsay) for supporting this work. IDRIS (Project No. 061616) is also acknowledged for allowance of computational time.

[1] C. Kaes, A. Katz, M. W. Hosseini, *Chem. Rev.* **2000**, *100*, 3553–3590.
[2] C. Piguet, G. Bernardinelli, G. Hopfgartner, *Chem. Rev.* **1997**, *97*, 2005–2062.
[3] U. Knof, A. von Zelewsky, *Angew. Chem.* **1999**, *111*, 312–333; *Angew. Chem. Int. Ed.* **1999**, *38*, 303–322, .
[4] P. Belser, S. Bernhard, E. Jandrasics, A. von Zelewsky, L. DeCola, V. Balzani, *Coord. Chem. Rev.* **1997**, *159*, 1–8.
[5] M. D. Ward, C. M. White, F. Barigelletti, N. Armaroli, G. Calogero, L. Flamigni, *Coord. Chem. Rev.* **1998**, *171*, 481–488.
[6] V. Balzani, A. Juris, M. Venturi, S. Campagna, S. Serroni, *Chem. Rev.* **1996**, *96*, 759–833.
[7] K. Kalyanasundaram, M. Gratzel, *Coord. Chem. Rev.* **1998**, *177*, 347–414.
[8] J. M. Lehn, *Rep. Prog. Phys.* **2004**, *67*, 249–265.
[9] J. R. Nitschke, J. M. Lehn, *Proc. Natl. Acad. Sci. USA* **2003**, *100*, 11970–11974.
[10] M. Ruben, J. Rojo, F. J. Romero-Salguero, L. H. Uppadine, J. M. Lehn, *Angew. Chem.* **2004**, *116*, 3728–3747; *Angew. Chem. Int. Ed.* **2004**, *43*, 3644–3662, .
[11] D. J. Cram, J. M. Cram, *Container Molecules and their Guests*, RSC, Cambridge, **1994**.
[12] D. B. Amabilino, J. F. Stoddart, *Chem. Rev.* **1995**, *95*, 2725–2828.
[13] J.-P. Sauvage, *Molecular Catenanes, Rotaxanes and Knots*, Wiley-VCH, Weinheim, **1999**.
[14] T. J. Hubin, A. G. Kolchinski, A. L. Vance, D. H. Busch, *Adv. Supramol. Chem.* **1999**, *6*, 237.
[15] D. M. D′Alessandro, F. R. Keene, *Chem. Rev.* **2006**, *106*, 2270–2298.
[16] K. B. Dillon, F. Mathey, J. F. Nixon, *Phosphorus: The Carbon Copy*, Wiley, Chichester, **1998**.
[17] P. Le Floch, *Coord. Chem. Rev.* **2006**, *250*, 627–681.
[18] F. Mathey in *Phosphorus-Carbon Heterocyclic Chemistry: The Rise of a New Domain* (Ed.: F. Mathey), Pergamon, Amsterdam, **2001**, p. 1.
[19] A. Breque, C. C. Santini, F. Mathey, J. Fischer, A. Mitschler, *Inorg. Chem.* **1984**, *23*, 3463–3467.
[20] J. M. Alcaraz, A. Breque, F. Mathey, *Tetrahedron Lett.* **1982**, *23*, 1565–1568.
[21] B. Schmid, L. M. Venanzi, A. Albinati, F. Mathey, *Inorg. Chem.* **1991**, *30*, 4693–4699.
[22] B. Schmid, L. M. Venanzi, T. Gerfin, V. Gramlich, F. Mathey, *Inorg. Chem.* **1992**, *31*, 5117–5122.
[23] P. Le Floch, *Phosphorus-Carbon Heterocyclic Chemistry: The Rise of a New Domain* (Ed.: F. Mathey), Pergamon, Amsterdam, **2001**, p. 485.
[24] P. Le Floch, D. Carmichael, L. Ricard, F. Mathey, *J. Am. Chem. Soc.* **1991**, *113*, 667–669.
[25] S. Holand, L. Ricard, F. Mathey, *J. Org. Chem.* **1991**, *56*, 4031–4035.
[26] P. Le Floch, D. Carmichael, L. Ricard, F. Mathey, *J. Am. Chem. Soc.* **1993**, *115*, 10665–10670.
[27] H. Trauner, P. Le Floch, J. M. Lefour, L. Ricard, F. Mathey, *Synthesis* **1995**, 717–726.
[28] P. Le Floch, L. Ricard, F. Mathey, *Bull. Soc. Chim. Fr.* **1994**, *131*, 330–334.
[29] P. Rosa, N. Mezailles, F. Mathey, P. Le Floch, *J. Org. Chem.* **1998**, *63*, 4826–4828.
[30] P. Le Floch, D. Carmichael, L. Ricard, F. Mathey, A. Jutand, C. Amatore, *Organometallics* **1992**, *11*, 2475–2479.
[31] P. Rosa, N. Mezailles, L. Ricard, F. Mathey, P. Le Floch, *Angew. Chem.* **2000**, *112*, 1893–1896; *Angew. Chem. Int. Ed.* **2000**, *39*, 1823–1826.
[32] P. Rosa, L. Ricard, P. Le Floch, F. Mathey, G. Sini, O. Eisenstein, *Inorg. Chem.* **1998**, *37*, 3154–3158.

[33] P. Le Floch, N. Maigrot, L. Ricard, C. Charrier, F. Mathey, *Inorg. Chem.* **1995**, *34*, 5070–5072.
[34] F. Hartl, T. Mahabiersing, P. Le Floch, F. Mathey, L. Ricard, P. Rosa, S. Zalis, *Inorg. Chem.* **2003**, *42*, 4442–4455.
[35] M. J. Bakker, F. W. Vergeer, F. Hartl, K. Goubitz, J. Fraanje, P. Rosa, P. Le Floch, *Eur. J. Inorg. Chem.* **2000**, 843–845.
[36] M. J. Bakker, F. W. Vergeer, F. Hartl, P. Rosa, L. Ricard, P. Le Floch, M. J. Calhorda, *Chem. Eur. J.* **2002**, *8*, 1741–1752.
[37] P. Rosa, N. Mezailles, L. Ricard, F. Mathey, P. Le Floch, Y. Jean, *Angew. Chem.* **2001**, *113*, 1291–1293; *Angew. Chem. Int. Ed.* **2001**, *40*, 1251–1253, .
[38] P. Rosa, L. Ricard, F. Mathey, P. Le Floch, *Organometallics* **2000**, *19*, 5247–5250.
[39] P. Rosa, L. Ricard, F. Mathey, P. Le Floch, *Organometallics* **1999**, *18*, 3348–3352.
[40] P. Le Floch, S. Mansuy, L. Ricard, F. Mathey, A. Jutand, C. Amatore, *Organometallics* **1996**, *15*, 3267–3274.
[41] H. Perron, A. Moores, I. Demachy, A. Lledos, Y. Jean, P. Le Floch, *New J. Chem.* **2004**, *28*, 838–842.
[42] N. Mézailles, P. Rosa, L. Ricard, F. Mathey, P. Le Floch, *Organometallics* **2000**, *19*, 2941–2943.
[43] P. Le Floch, D. Carmichael, F. Mathey, *Phosphorus Sulfur Silicon Relat. Elem.* **1993**, *76*, 255.
[44] S. Choua, H. Sidorenkova, T. Berclaz, M. Geoffroy, P. Rosa, N. Mezailles, L. Ricard, F. Mathey, P. Le Floch, *J. Am. Chem. Soc.* **2000**, *122*, 12227–12234.
[45] S. Herzog, R. Taube, *Z. Chem.* **1962**, *2*, 208–214.
[46] M. Kaupp, T. Kopf, A. Murso, D. Stalke, C. Strohmann, J. R. Hanks, F. G. N. Cloke, P. B. Hitchcock, *Organometallics* **2002**, *21*, 5021–5028.
[47] C. K. Jörgensen, *Oxidation Numbers and Oxidation States*, Springer, Berlin, **1969**, p. 213.
[48] M. D. Ward, J. A. McCleverty, *J. Chem. Soc. Dalton Trans.* **2002**, 275–288.
[49] D. Herebian, E. Bothe, E. Bill, T. Weyhermuller, K. Wieghardt, *J. Am. Chem. Soc.* **2001**, *123*, 10012–10023.
[50] R. Hoffmann, J. M. Howell, A. R. Rossi, *J. Am. Chem. Soc.* **1976**, *98*, 2484–2492.
[51] M. Kaupp, *Angew. Chem.* **2001**, *113*, 3642–3677; *Angew. Chem. Int. Ed.* **2001**, *40*, 3534–3565, .
[52] K. Seppelt, *Acc. Chem. Res.* **2003**, *36*, 147–153.
[53] S. K. Kang, T. A. Albright, O. Eisenstein, *Inorg. Chem.* **1989**, *28*, 1611–1613.
[54] Here the labels are given according to the highest possible symmetry for the limit and intermediate structures (see Scheme 3).
[55] D. L. Kepert, *Inorg. Chem.* **1972**, *11*, 1561–1563.
[56] S. Alvarez, D. Avnir, M. Llunell, M. Pinsky, *New J. Chem.* **2002**, *26*, 996–1009.
[57] Gaussian 03, Revision C.02, M. J. Frisch, G. W. Trucks, H. B. Schlegel, G. E. Scuseria, M. A. Robb, J. R. Cheeseman, J. A. Montgomery, Jr., T. Vreven, K. N. Kudin, J. C. Burant, J. M. Millam, S. S. Iyengar, J. Tomasi, V. Barone, B. Mennucci, M. Cossi, G. Scalmani, N. Rega, G. A. Petersson, H. Nakatsuji, M. Hada, M. Ehara, K. Toyota, R. Fukuda, J. Hasegawa, M. Ishida, T. Nakajima, Y. Honda, O. Kitao, H. Nakai, M. Klene, X. Li, J. E. Knox, H. P. Hratchian, J. B. Cross, V. Bakken, C. Adamo, J. Jaramillo, R. Gomperts, R. E. Stratmann, O. Yazyev, A. J. Austin, R. Cammi, C. Pomelli, J. W. Ochterski, P. Y. Ayala, K. Morokuma, G. A. Voth, P. Salvador, J. J. Dannenberg, V. G. Zakrzewski, S. Dapprich, A. D. Daniels, M. C. Strain, O. Farkas, D. K. Malick, A. D. Rabuck, K. Raghavachari, J. B. Foresman, J. V. Ortiz, Q. Cui, A. G. Baboul, S. Clifford, J. Cioslowski, B. B. Stefanov, G. Liu, A. Liashenko, P. Piskorz, I. Komaromi, R. L. Martin, D. J. Fox, T. Keith, M. A. Al-Laham, C. Y. Peng, A. Nanayakkara, M. Challacombe, P. M. W. Gill, B. Johnson, W. Chen, M. W. Wong, C. Gonzalez, J. A. Pople, Gaussian, Inc., Wallingford, CT, **2004**.
[58] R. G. Parr, W. Yang, *Density Functional Theory of Atoms and Molecules*, Oxford University Press, Oxford, UK, **1989**.
[59] T. Ziegler, *Chem. Rev.* **1991**, *91*, 651–667.
[60] C. T. Lee, W. T. Yang, R. G. Parr, *Phys. Rev. B* **1988**, *37*, 785–789.
[61] A. D. Becke, *J. Chem. Phys.* **1993**, *98*, 5648–5652.
[62] P. J. Stephens, F. J. Devlin, C. F. Chabalowski, M. J. Frisch, *J. Phys. Chem.* **1994**, *98*, 11623–11627.
[63] P. J. Hay, W. R. Wadt, *J. Chem. Phys.* **1985**, *82*, 299–310.
[64] W. R. Wadt, P. J. Hay, *J. Chem. Phys.* **1985**, *82*, 284–298.
[65] A. Hollwarth, M. Bohme, S. Dapprich, A. W. Ehlers, A. Gobbi, V. Jonas, K. F. Kohler, R. Stegmann, A. Veldkamp, G. Frenking, *Chem. Phys. Lett.* **1993**, *208*, 237–240.
[66] M. M. Francl, W. J. Pietro, W. J. Hehre, J. S. Binkley, M. S. Gordon, D. J. Defrees, J. A. Pople, *J. Chem. Phys.* **1982**, *77*, 3654–3665.
[67] W. J. Hehre, R. Ditchfie, J. A. Pople, *J. Chem. Phys.* **1972**, *56*, 2257–2261.
[68] S. I. Gorelsky, http://www.sg-chem.net/ed, York University, Toronto, Canada, **1997**.
[69] S. I. Gorelsky, A. B. P. Lever, *J. Organomet. Chem.* **2001**, *635*, 187–196.
[70] P. Rosa, PhD thesis, Ecole Polytechnique (Palaiseau), **2000**.
[71] Additional calculations were performed on the **1N**–**3N** minima with polarization functions on the metal center (A. W. Ehlers, M. Bohme, S. Dapprich, A. Gobbi, A. Hollwarth, V. Jonas, K. F. Kohler, R. Stegmann, A. Veldkamp, G. Frenking, *Chem. Phys. Lett.* **1993**, *208*, 111–114) and on the carbon atoms (6-31G* basis set). The average M–N distances are shortened by less than 0.010 Å (2.109, 2.249, and 2.211 Å instead of 2.110, 2.257, and 2.218 Å for **1N**, **2N**, and **3N**, respectively), and the central C–C distance of the bpy ligands by less than 0.005 Å (1.396, 1.391, 1.388 Å instead of 1.398, 1.395, and 1.391 Å for **1N**, **2N**, and **3N**, respectively).
[72] P. Rosa, N. Mezailles, L. Ricard, F. Mathey, P. Le Floch, *Angew. Chem.* **2001**, *113*, 4608–4611; *Angew. Chem. Int. Ed.* **2001**, *40*, 4476–4479, .
[73] In idealized D_{3h} symmetry, these orbitals would be of different symmetry (a_1' for z^2 and a_2' for π^*), so that their overlap would rigorously vanish. Therefore it is the $D_{3h} \rightarrow C_{3h}$ symmetry lowering which allows this stabilizing interaction in the TP structure of **2P**.
[74] In a doubly occupied MO developed both on the metal (x%) and the ligands ((100−x)%), the numbers of electrons attributed to the metal and the ligands are (2x/100) and (2(100−x)/100), respectively
[75] Note that the energetic evolution of individual MOs may be more difficult to rationalize in DFT (or ab initio) calculations than in monoelectronic methods. In fact, the energy variations in extended Hückel calculations are due to changes in the bonding or antibonding interactions in the MO or polarization effects. In DFT or ab initio calculations, the energy of a given orbital may well vary even if its shape is kept unchanged.
[76] Additional calculations were performed with f polarization functions on the metal center to test their influence on the OC/TP preference. Complexes **1N**–**3N** (OC, for M = Ti, Zr, and Hf, respectively) and **1N′**–**3N′** (TP, for M = Ti, Zr and Hf, respectively) were reoptimized with a set of f polarization functions on the metal center (A. W. Ehlers, M. Bohme, S. Dapprich, A. Gobbi, A. Hollwarth, V. Jonas, K. F. Kohler, R. Stegmann, A. Veldkamp, G. Frenking, *Chem. Phys. Lett.* **1993**, *208*, 111–114). The energy difference between the OC and TP minima is only slightly perturbed (ΔE = 13.9, 4.1, and 7.1 kcal mol^{-1} with f functions instead of 13.6, 3.8, and 6.9 kcal mol^{-1} without f functions for M = Ti, Zr, and Hf, respectively).
[77] These sets of degenerate e ligand orbitals are the HOMO−3 and HOMO−4 on the one hand (7.1%) and the HOMO−6 and HOMO−7 on the other (14.0%).
[78] E. Larsen, G. N. Lamar, B. E. Wagner, R. H. Holm, J. E. Parks, *Inorg. Chem.* **1972**, *11*, 2652–2668.

Received: August 10, 2006
Published online: December 18, 2006

